

Development and Validation of Resistance-Capacitance Model for Phase Change Material Embedded in Porous Media

Tanjebul Alam

Dept. of Mechanical Engineering
University of Maryland
College Park, MD, USA
talam@umd.edu

Daniel Bacellar

Dept. of Mechanical Engineering
University of Maryland
College Park, MD, USA
dfbace@umd.edu

Jiazhen Ling

Dept. of Mechanical Engineering
University of Maryland
College Park, MD, USA
jiazhen@umd.edu

Vikrant Aute

Dept. of Mechanical Engineering
University of Maryland
College Park, MD, USA
vikrant@umd.edu

Abstract— A simple and effective way to enhance PCM thermal conductivity is by embedding porous materials with high thermal conductivities. In this work, CFD was used to evaluate the melting of PCM embedded in metal foam supplied with constant heat flux. Good agreement between experimental and numerical results has been found with a mean PCM local temperature deviation of 1.62K and 2.97K in two locations. The CFD simulation time was 56 hours for 6.5 hours of flow time. A computationally efficient resistance capacitance-based model (RCM) was developed to improve simulation speed. The proposed RCM exhibited mean local temperature deviations of 1.86K and 2.96K when compared against the experimental data for two thermocouple positions, however, it was approximately 2.5×10^5 times faster than CFD. The charging time deviation was less than 1% compared to CFD, and no significant change in thermal energy stored was observed since the temperature differences were small enough to result in insignificant sensible heat deviation. A simulation cost-effectiveness index (CEI) considering accuracy and computational affordability was introduced; the CEI of the RCM solver is 10^3 times better compared to CFD for the prediction of local PCM temperature.

Keywords—PCM, CFD, resistance-capacitance model, computational cost

I. INTRODUCTION

Despite having high energy density, achieving desired power density can be a major challenge in PCM heat exchangers due to the low thermal conductivity of PCM materials. To increase the heat transfer rate, different techniques such as using metal fins, adding heat pipes, using high conductive nanoparticles, embedding PCM in graphite or metal foams have been widely explored by researchers[1]–[3]. Among these techniques, adding metal foam has shown promise of being an efficient way to improve the thermal conductivity of PCM as it offers a large surface-area-to-volume ratio, high porosity, high thermal conductivity, is lightweight, and have relatively low cost.

The objectives of metal foam composite PCMHXs should be to maximize thermal conductivity enhancement while minimizing the amount of PCM volume that is replaced by

porous material. A study by Sedeh and Khodadadi [4] achieved an effective thermal conductivity of up to 30 W/m-K with a graphite matrix in comparison with the thermal conductivity of 0.13 W/m-K of the PCM. But the volume fraction of the graphite matrix was high (25%) which reduced the effective thermal storage energy density. Cui [5] reported a heat transfer rate enhancement of 36% by using a low volume fraction (4%) of copper foam. Fleming *et al.* [6] tested a tube bundle-type exchanger which was immersed in an aluminum foam (volume fraction of 5.4%) impregnated with PCM (water). It was compared to the tube bundle exchanger without the metal foam and was found that, during solidification, the metal enhancement increased the overall heat transfer coefficient (HTC) by 20%. For the melting, the overall HTC was found to be increased by 100%. The study also suggested that increasing the surface area and distribution uniformity of the metal foam (reducing the pore size of foam while maintaining a particular volume fraction) can provide a more homogenous system with higher effective thermal conductivity.

CFD simulation can be a very powerful tool for understanding detailed thermal characteristics of metal foam composite PCMHX and their development because of the prediction accuracy mentioned in different works of literature [7]–[10]. However, it has been shown by Alam *et al.* [11] that CFD can be computationally expensive and the simulation time can take 50x more compared to the experiment time. For larger-scale simulations, e.g., heat exchanger optimization, this can be prohibitive. Bacellar *et al.* [12]–[13] presented a reduced-order model using CFD-based correlations and reduced-order domain for faster evaluation of thermal energy storage devices. The results showed a great match to the CFD simulations with 4 to 5 orders of magnitude less computational cost compared to CFD. But generating correlations that cover a large design space can still be computationally expensive. Therefore, a simpler, lighter-weight, tool is needed.

Simplified models for PCM storages have been developed based on resistances and capacitances (RCM) by researchers. Several RCM for various applications can be found in literature

[14]–[18]. The models are mainly 1D and only takes conduction as the heat transfer mode. In these literatures, the thermal resistance is constant. However, due to free convection of the liquid PCM during the melting process, decreasing of the thermal resistance may need to be considered for some configurations. However proper approximation of the effect of natural convection may need the usage of computationally expensive numerical methods to develop correlations, which defeats the purpose of using RCM. Neumann *et al.* [19] proposed a simplified 1D RCM which was developed with considering free convection during the melting process in rectangular PCM gaps based on correlations proposed by Vogel *et al.* [20]; the model was verified against the CFD model. The study showed that the mean deviation of the outlet fluid temperature and PCM temperature between both models was 0.62 K and 0.85 K, respectively. The simulation time for the RCM was reduced by a factor of 20-30 compared to CFD. The study considered a geometry where the motion of liquid PCM is significant, but for structured designs, the natural convection effect can be less dominant and be dismissed in favor of computational speed gains.

To the best of our knowledge, no study has previously utilized RCM to model composite PCM with metal foam. In this study, a computationally inexpensive RCM has been developed for the melting of PCM embedded in metal foam supplied with constant heat flux. The model is validated against experimental data from literature and then compared against a validated CFD model. The prediction difference in local temperature profile, energy storage, and melting time between the two models is discussed in this paper along with the respective computational costs.

II. MODEL DESCRIPTION

A. Subject of Study

Melting in paraffin-based PCM impregnated with copper, the foam has been tested experimentally by Zheng *et al.* [21]. The composite PCM of porosity (ratio of PCM volume and total volume) 0.95 was utilized in the melting experiment. The metal foam pore size was 5 Pores Per Inch (PPI). Figure 1a shows the composite PCM with the dimension of 100×100×30 mm. It was heated with a 100×10×30 mm electrical heater attached to the top of the PCM enclosure, which provided constant and uniform heat flux. All the other walls are considered adiabatic in the model. Three thermocouples A, B & C were placed at 25, 50, and 100 mm away from the heated wall respectively, as shown in Figure 1b. The thermophysical properties of PCM and copper foam are provided in Table I.

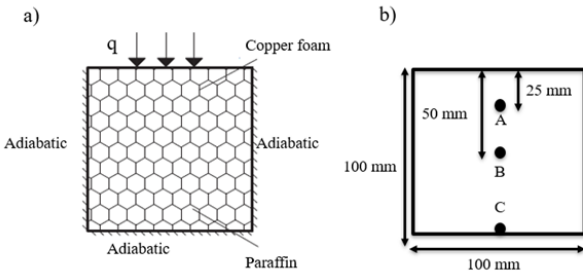


Fig. 1. a) Composite PCM setup with metal foam b) Thermocouple positions

TABLE I. THERMOPHYSICAL PROPERTIES OF PCM AND COPPER FOAM [21]

Properties	Paraffin	Copper Foam
k (W/m-K)	0.3	380
ρ (kg/m ³)	900	8900
c_p (J/kg-K)	2300	386
$T_{sol} - T_{melt}$ (K)	323-331	-
h_s (J/kg)	148,800	-
μ (Pa-s)	0.00324	-
β (K ⁻¹)	0.0005	-

B. CFD Model

A 2D numerical simulation was carried out in ANSYS FLUENT. Natural convection was taken into consideration during the PCM melting process using the Boussinesq approximation. Structured grid was used to discretize the computational domain, containing 10,000 elements. The porous media model of ANSYS Fluent was used to model the composite PCM. The inertial and viscous resistance parameters were calculated by using equations referenced in Zheng *et al.* [21]. Time step size was fixed in 0.5s based on a similar CFD study by Zhang *et al.*[8]. The initial temperature was 287K and a constant heat flux (1150W/m²) was applied on the top wall. All the other walls were assumed adiabatic. The effective thermal conductivity was calculated (2.28 W/m-K) from the equations provided by Esapour *et al.* [10]. The mushy zone parameter was selected as 10⁵ and 30 iterations per time step were used. The other CFD settings are provided in Table II.

TABLE II. CFD SETTINGS FOR MELTING IN COMPOSITE PCM WITH METAL FOAM

Pressure-Velocity Coupling	Transient Formulation	Momentum Discretization Scheme	Energy Discretization Scheme
SIMPLE	2 nd order implicit	2 nd order upwind	2 nd order upwind
Pressure Discretization Scheme	x, y-velocity Convergence Criteria	Continuity Convergence Criteria	Energy Convergence Criteria
Presto	10 ⁻⁵	10 ⁻⁵	10 ⁻¹²

C. Resistance Capacitance Model (RCM)

The RCM is lightweight compared to CFD as it does not solve higher-order physics but still can provide good accuracy using an approximation of the thermal resistance at a very low computational cost. Figure 2 shows the thermal network of heat flow in the RCM representation of the physical model. The computational domain is discretized into equal-length segments and each of the segments has individual resistance and capacitance. The assumptions in the RCM model are:

- All segments have uniform porosity, heat capacity, and thermal resistance.

- Thermal conductivity, specific heat, and density of solid and liquid PCM are assumed to be equal
- Effects of natural convection are negligible and heat transfer is conduction-dominated
- No heat loss through the walls (adiabatic)
- No mass transfer in between segments

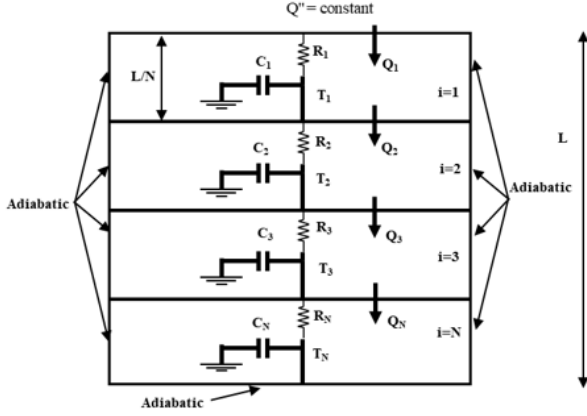


Fig. 2. Thermal network of 1D RCM for composite PCM

The thermal network parameters can be calculated with a simple explicit time-marching formulation described in equations 1-7.

$$\dot{Q}_{i,t} = \dot{Q}'' \cdot A; i = 1 \quad (1)$$

$$\dot{Q}_{i,t} = \frac{T_{i-1,t} - T_{i,t}}{R_{i-1,t}}; i \geq 2 \quad (2)$$

$$\frac{dT_{i,t+1}}{dt} = \frac{\dot{Q}_{i,t} - \dot{Q}_{i+1,t}}{C_{i,t}} \quad (3)$$

$$T_{i,t+\Delta t} = T_{i,t} + \frac{dT_{i,t}}{dt} \cdot \Delta t \quad (4)$$

$$R_{i,t} \approx R_{cond} = \frac{L/N}{k_{eff} \cdot A}; R_{nat_conv} \ll R_{cond} \quad (5)$$

$$C_{PCM} = \begin{cases} c_{p,s} & \text{for } T \leq T_{sol} \\ c_{p,s} + \frac{h_s}{T_{melt} - T_{sol}} & \text{for } T_{sol} < T < T_{melt} \\ c_{p,l} & \text{for } T \geq T_{melt} \end{cases} \quad (6)$$

$$C_{i,t} = [\gamma C_{PCM} \rho_{PCM} + (1-\gamma)C_{FOAM} \rho_{FOAM}] V \quad (7)$$

Where, i denotes a specific segment and t denotes a specific time step. Total volume of a segment is denoted by V, area of a segment is A and total height of the domain is L. The domain is

discretized into N number of equal length segments. $R_{i,t}$, $C_{i,t}$, $Q_{i,t}$, $T_{i,t}$ represents the thermal resistance, thermal capacitance, heat flow and temperature of a specific segment at a specific time. PCM porosity, γ , is 95%, β represents the liquid fraction, ρ , the density, and k_{eff} is the effective thermal conductivity. For the latter, the same value from CFD is used in RCM.

Figure 3 shows the solver flow chart for the RCM. The PCM properties, geometry description, discretization information, boundary and initial conditions are taken as input for the model and the temperature at different segments are the output from solver.

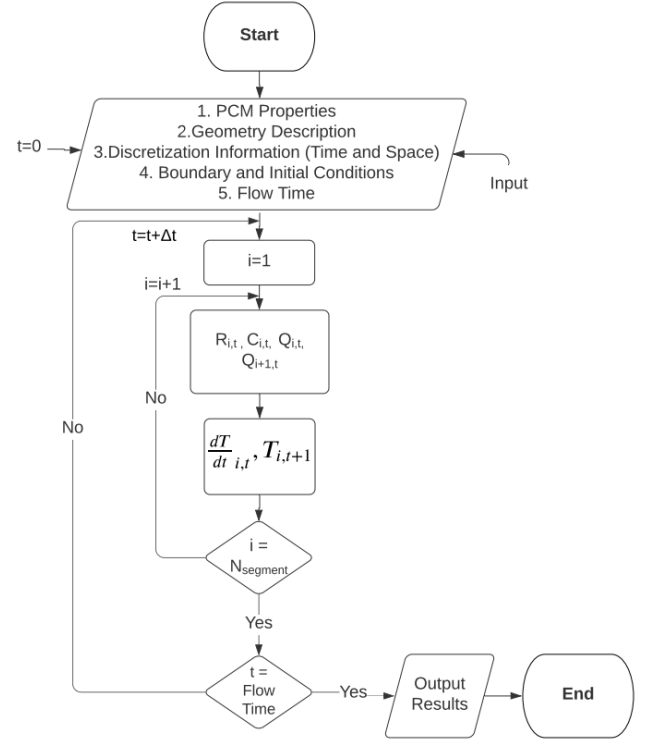


Fig. 3. Solver flowchart for the RCM

Figure 4 and 5 show the grid size and the time step independency of RCM, respectively. Other than one very large segment size number, all the other grid sizes show the similar result. We use 10 segments and 2s time step size in this work.

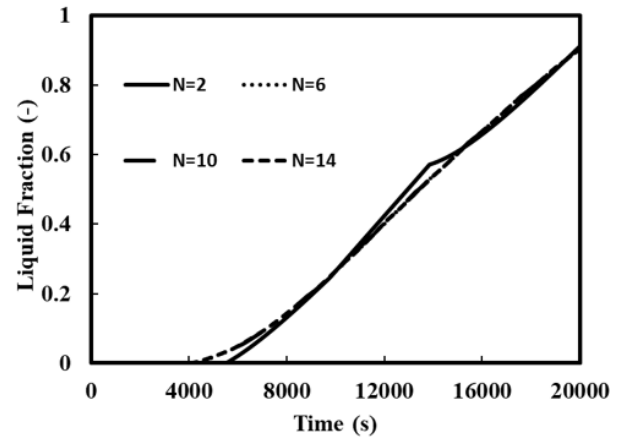


Fig. 4. Grid independence analysis

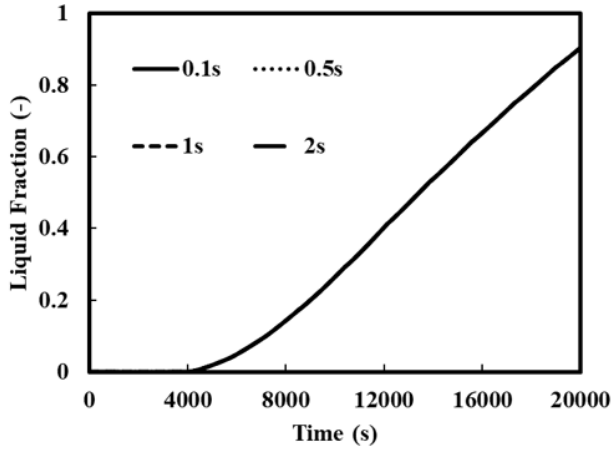


Fig. 5. Time-step independence analysis

III. RESULTS

Two thermocouples A and C were placed at 25 and 100 mm away from the heated wall in the experimental setup. The temperature profile in these two points for experiment and CFD simulation have been compared with RCM results in Figure 6. The plots show that the RCM results are matching very well with both the experimental and CFD results. The mean deviations of CFD and experimental temperature are found to be 1.62K and 2.97K for thermocouples A and C, respectively. For RCM and experimental temperature, the mean deviations are 1.84K and 2.96K for thermocouples A and C, respectively. The plots validate both CFD and RCM for the composite PCM..

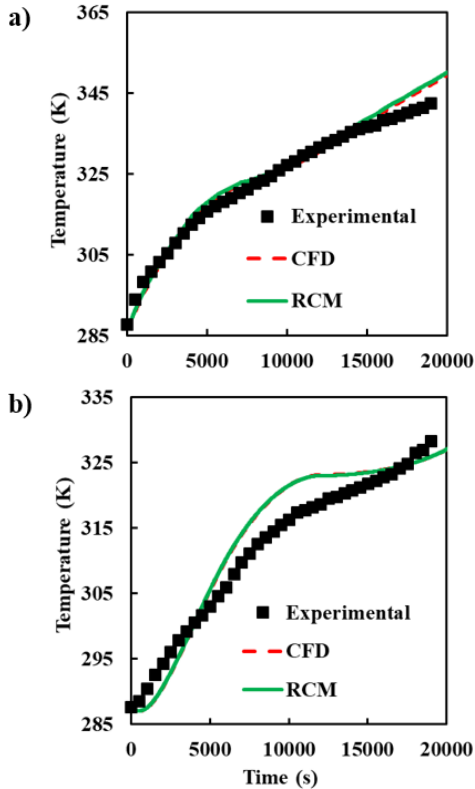


Fig. 6. Comparison of RCM results with experiment and CFD for a) thermocouple A b) thermocouple C

The deviation in the predicted temperature for TC C is higher in both RCM and CFD compared to TC A. This can be attributed to the adiabatic wall condition assumed in the model although there is heat loss to the ambient in the experiment. The hypothesis is that at the beginning of the simulation when the PCM temperature is lower (below ambient), the model is not considering the heat coming in from ambient and so it is underpredicting the temperature. Once the PCM temperature rises higher than the ambient the model is not considering the heat loss and so overpredicting the temperature.

Figure 6 shows the comparison of RCM results with CFD results for average PCM temperature and liquid fraction. The plots show that the results from RCM are matching almost exactly with CFD.

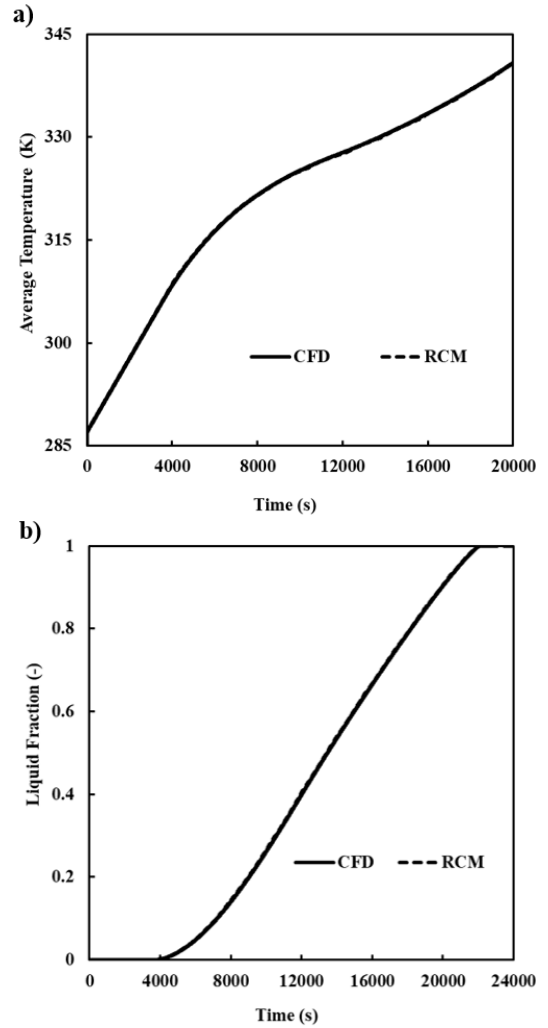


Fig. 7. Comparison of RCM results with CFD for a) average PCM temperature b) liquid fraction

For every time step, a liquid fraction for each segment in RCM can be calculated based on equation 8 and equation 9 can be used for the average liquid fraction for the whole domain.

$$\beta_{i,t} = \frac{T_{i,t} - T_{sol}}{T_{melt} - T_{sol}} \quad (8)$$

$$\beta_{avg,t} = \frac{\sum_{i=1}^N \beta_{i,t}}{N} \quad (9)$$

Table III shows the hardware information of the computer and Table IV compares computational cost and accuracy of melting time, energy storage, and local temperature prediction between RCM and CFD. Here, the real-time factor is the ratio between the time required for simulation and experimental time and is denoted by α . The results for RCM are based on 0.5s time step to compare against CFD results with same time step. However, with a higher time step size of 2s, the model is also similarly accurate with even lower computational cost. (Figure 5)

The experimental energy storage is a theoretical calculation for a constant heat flux in PCM domain with no heat loss for 19,800s. The energy storage for both RCM and CFD is calculated using the average PCM domain temperature (T_{avg}) with equation 10.

$$E_t = \begin{cases} (m_{PCM} + m_{foam})(T_{avg} - T_i) & \text{for } T_{avg} \leq T_{sol} \\ m_{PCM} h_s \frac{T_{avg} - T_{sol}}{T_{melt} - T_{sol}} + m_{foam}(T_{avg} - T_{sol}) & \text{for } T_{sol} < T_{avg} < T_{melt} \\ (m_{PCM} + m_{foam})(T_{avg} - T_{melt}) & \text{for } T_{avg} \geq T_{melt} \end{cases} \quad (10)$$

The table shows that, both CFD and RCM predicted the energy storage with a deviation of around 0.8% when compared to experimental energy storage. In both CFD and RCM, the time needed for liquid fraction to go to 1 is considered as melting time. Ensuring this is difficult in an experimental study and it is possible to visually consider a case fully melted before it completely melts. The table also demonstrates that, with a deviation of less than 1%, the RCM can predict the melting time similar to CFD with 10^5 order of speed gain.

Mean absolute temperature deviation is denoted by σ_{Temp} and temperature deviation factor is denoted by σ_F . Here, we will introduce a cost-effectiveness index (CEI) to compare the tradeoff between different models for transient simulations. The index will be calculated based on equation 12. If the deviation between two models is considered acceptable, then the lower the value of CEI is for a model, the better its performance.

$$\sigma_{Temp} = \frac{\sum_{n=1}^n |T_{exp,t} - T_{sim,t}|}{n} \quad (11)$$

$$n = \frac{a-b}{\Delta t} \quad (12)$$

$$\sigma_F = \frac{\sigma_{Temp}}{T_{max} - T_{min}} \quad (13)$$

$$CEI = \frac{1}{\alpha \times \sigma_F} \quad (14)$$

TABLE III. COMPUTER HARDWARE INFORMATION

Number of Cores	Processor	RAM (Gigabyte)
28	2 x Intel® Xeon® Gold 5117, 2.00 GHz	96

TABLE IV. COMPARISON OF COMPUTATIONAL COST AND ACCURACY BETWEEN CFD AND RCM

Parameter	Experimental	CFD	RCM
Run Time (s)	23,400	201,600	1.2
Time Step (s)	-	0.5	0.5
α	1	8.61	5.13×10^{-5}
Time for $\beta=1$	NA	22,067	22,008
Energy Storage (kJ)	68.31	67.72	67.7
Absolute Deviation for Energy Storage (%)	-	0.86	0.88
σ_{Temp} at A (K)	-	1.62	1.84
σ_{Temp} at C (K)	-	2.97	2.96

Based on Table IV, for temperature prediction at point A, the CEI for CFD is 4. The CEI for RCM is 10593.22 which is 2.648×10^3 times better than CFD. The CEI can also be calculated based on the absolute deviation for energy storage also.

The CEI along with the figures and the table provided above show that for a composite PCMHX, with a good estimation of thermal conductivity of composite, CFD is not needed as RCM can predict with excellent accuracy with significant speed gain. This also validates our assumption of neglecting the effects of natural convection in a metal foam composite PCM and shows that diffusion-based solvers can predict the thermal characteristics of a PCMHX with structured enhancement accurately.

IV. CONCLUSION

A CFD and a lightweight resistance-capacitance model (RCM) have been developed for the melting of composite PCM with constant heat flux. Both have been validated against experimental data from literature and show good prediction capability of local temperature. However, the RCM was able to provide prediction accurately with 10^5 order of speed gain. A cost-effective index was introduced which showed the performance of RCM was 2.648×10^3 times better as the accuracy penalty is almost negligible compared to the significant speed gain. This makes RCM suitable for large-scale simulations such as optimized designs of PCMHX.

NOMENCLATURE

- a Experiment start time (s)
- b Experiment end time (s)
- $c_{p,s}$ Solid specific heat (J/kg-K)
- $c_{p,l}$ Liquid specific heat (J/kg-K)

h_s	Latent heat (J/kg)
k	Thermal conductivity (W/m-K)
L	PCM domain length (m)
m	mass (kg)
N	Number of segments (-)
n	Number of points evaluated for σ_{Temp} (-)
T_{sol}	Solidification temperature (K)
T_{melt}	Liquidous temperature (K)
T_{exp}	Experimental temperature (K)
T_{sim}	Simulation temperature (K)
T_{max}	Maximum temperature in experiment (K)
T_{min}	Minimum temperature in experiment (K)
TC	Thermocouple
Δt	Time-step size for σ_{Temp} (s)
α	Real-time factor (-)
β	Thermal Expansion coefficient (K^{-1})
γ	Porosity (-)
ρ	Density (kg/m^3)
μ	Viscosity (Pa-s)

ACKNOWLEDGMENT

The authors would like to acknowledge the support from the Modeling and Optimization Consortium (MOC) at the Center for Environmental Energy Engineering (CEEE), University of Maryland, College Park.

REFERENCES

- [1] L. Fan and J. M. Khodadadi, "Thermal conductivity enhancement of phase change materials for thermal energy storage: A review," *Renew. Sustain. Energy Rev.*, vol. 15, no. 1, pp. 24–46, 2011, doi: 10.1016/j.rser.2010.08.007.
- [2] N. I. Ibrahim, F. A. Al-Sulaiman, S. Rahman, B. S. Yilbas, and A. Z. Sahin, "Heat transfer enhancement of phase change materials for thermal energy storage applications: A critical review," *Renew. Sustain. Energy Rev.*, vol. 74, no. February, pp. 26–50, 2017, doi: 10.1016/j.rser.2017.01.169.
- [3] R. Elarem *et al.*, "A comprehensive review of heat transfer intensification methods for latent heat storage units," *Energy Storage*, no. December, pp. 1–30, 2020, doi: 10.1002/est2.127.
- [4] M. Moeini Sedeh and J. M. Khodadadi, "Thermal conductivity improvement of phase change materials/graphite foam composites," *Carbon N. Y.*, vol. 60, pp. 117–128, 2013, doi: 10.1016/j.carbon.2013.04.004.
- [5] H. T. Cui, "Experimental investigation on the heat charging process by paraffin filled with high porosity copper foam," *Appl. Therm. Eng.*, vol. 39, pp. 26–28, 2012, doi: 10.1016/j.applthermaleng.2012.01.037.
- [6] E. Fleming, S. Wen, L. Shi, and A. K. Da Silva, "Experimental and theoretical analysis of an aluminum foam enhanced phase change thermal storage unit," *Int. J. Heat Mass Transf.*, vol. 82, pp. 273–281, 2015, doi: 10.1016/j.ijheatmasstransfer.2014.11.022.
- [7] F. Zhu, C. Zhang, and X. Gong, "Numerical analysis and comparison of the thermal performance enhancement methods for metal foam/phase change material composite," *Appl. Therm. Eng.*, vol. 109, pp. 373–383, 2016, doi: 10.1016/j.applthermaleng.2016.08.088.
- [8] P. Zhang, Z. N. Meng, H. Zhu, Y. L. Wang, and S. P. Peng, "Melting heat transfer characteristics of a composite phase change material fabricated by paraffin and metal foam," *Appl. Energy*, vol. 185, pp. 1971–1983, 2017, doi: 10.1016/j.apenergy.2015.10.075.
- [9] Z. Liu, Y. Yao, and H. Wu, "Numerical modeling for solid-liquid phase change phenomena in porous media: Shell-and-tube type latent heat thermal energy storage," *Appl. Energy*, vol. 112, pp. 1222–1232, 2013, doi: 10.1016/j.apenergy.2013.02.022.
- [10] M. Esapour, A. Hamzehnezhad, A. A. Rabienataj Darzi, and M. Jourabian, "Melting and solidification of PCM embedded in porous metal foam in horizontal multi-tube heat storage system," *Energy Convers. Manag.*, vol. 171, no. January, pp. 398–410, 2018, doi: 10.1016/j.enconman.2018.05.086.
- [11] T. Alam, D. Bacellar, J. Ling, and V. Aute, "Numerical Study and Validation of Melting and Solidification in PCM Embedded Heat Exchangers with Straight Tube," in *18th International Refrigeration and Air Conditioning Conference at Purdue*, 2021, pp. 1–8.
- [12] D. Bacellar, T. Alam, J. Ling, and V. Aute, "Automated Parameterized CFD Simulations of Phase-Change Material Embedded Heat Exchangers," *2021 20th IEEE Intersoc. Conf. Therm. Thermomechanical Phenom. Electron. Syst.*, pp. 538–543, 2021, doi: 10.1109/ITHERM51669.2021.9503249.
- [13] D. Bacellar, T. Alam, J. Ling, and V. Aute, "A Study on Computational Cost Reduction of Simulations of Phase-Change Material (PCM) Embedded Heat Exchangers," in *18th International Refrigeration and Air Conditioning Conference at Purdue*, 2021, pp. 1–9.
- [14] N. Zhu, S. Wang, X. Xu, and Z. Ma, "A simplified dynamic model of building structures integrated with shaped-stabilized phase change materials," *Int. J. Therm. Sci.*, vol. 49, no. 9, pp. 1722–1731, 2010, doi: 10.1016/j.ijthermalsci.2010.03.020.
- [15] A. Bontemps, M. Ahmad, K. Johanns, and H. Sallée, "Experimental and modelling study of twin cells with latent heat storage walls," *Energy Build.*, vol. 43, no. 9, pp. 2456–2461, 2011, doi: 10.1016/j.enbuild.2011.05.030.
- [16] J. Gao, T. Yan, T. Xu, Z. Ling, G. Wei, and X. Xu, "Development and experiment validation of variable-resistance-variable-capacitance dynamic simplified thermal models for shape-stabilized phase change material slab," *Appl. Therm. Eng.*, vol. 146, no. July 2018, pp. 364–375, 2019, doi: 10.1016/j.applthermaleng.2018.09.124.
- [17] A. Stupar, U. Drogenik, and J. W. Kolar, "Application of phase change materials for low duty cycle high peak load power supplies," *2010 6th Int. Conf. Integr. Power Electron. Syst. CIPS 2010*, pp. 16–18, 2011.
- [18] P. A. Mirzaei and F. Haghghat, "Modeling of phase change materials for applications in whole building simulation," *Renew. Sustain. Energy Rev.*, vol. 16, no. 7, pp. 5355–5362, 2012, doi:

10.1016/j.rser.2012.04.053.

- [19] H. Neumann, S. Gamisch, and S. Gschwander, "Comparison of RC-model and FEM-model for a PCM-plate storage including free convection," *Appl. Therm. Eng.*, vol. 196, no. September 2020, p. 117232, 2021, doi: 10.1016/j.applthermaleng.2021.117232.
- [20] J. Vogel, J. Felbinger, and M. Johnson, "Natural convection in high temperature flat plate latent heat thermal energy storage systems," *Appl. Energy*, vol. 184, pp. 184–196, 2016, doi: 10.1016/j.apenergy.2016.10.001.
- [21] H. Zheng, C. Wang, Q. Liu, Z. Tian, and X. Fan, "Thermal performance of copper foam/paraffin composite phase change material," *Energy Convers. Manag.*, vol. 157, no. September 2017, pp. 372–381, 2018, doi: 10.1016/j.enconman.2017.12.023.